EVIDENCE FOR RELATIVISTIC OUTFLOWS IN NARROW-LINE SEYFERT 1 GALAXIES

KAREN M. LEIGHLY

Columbia Astrophysics Laboratory, 538 West 120th Street, New York, NY 10027; leighly@ulisse.phys.columbia.edu

RICHARD F. MUSHOTZKY

Goddard Space Flight Center, Code 660.2, Greenbelt, MD 20770; mushotzky@lheavx.gsfc.nasa.gov

KIRPAL NANDRA[1]

Goddard Space Flight Center, Code 660.2, Greenbelt, MD 20770; nandra@lheavx.gsfc.nasa.gov

AND

KARL FORSTER

Department of Astronomy, Columbia University, 538 West 120th Street, New York, NY 10027; karlfor@mikado.columbia.edu

ABSTRACT

We report the observation of features near 1 keV in the *ASCA* spectra from three narrow-line Seyfert 1 (NLS1) galaxies. We interpret these as oxygen absorption in a highly relativistic outflow. If interpreted as absorption edges, the implied velocities are 0.2–0.3 c, near the limit predicted by "line-locking" radiative acceleration. If instead interpreted as broad absorption lines, the implied velocities are ~0.57 c, interestingly near the velocity of particles in the last stable orbit around a Kerr black hole, although a physical interpretation of this is not obvious. The features are reminiscent of the UV absorption lines seen in broad absorption line quasars (BALQSOs), but with larger velocities, and we note the remarkable similarities in the optical emission line and broadband properties of NLS1s and low-ionization BALQSOs.

Subject headings: galaxies: active —
galaxies: individual (IRAS 13224−3809, 1H 0707−495, PG 1404+226) — X-rays: galaxies

1. INTRODUCTION

Narrow-line Seyfert 1 galaxies (NLS1s) are defined by their optical line properties (see, e.g., Goodrich 1989): (1) the Balmer lines are only slightly broader than the forbidden lines (Hβ FWHM < 2000 km s^{-1}); (2) the forbidden line emission is relatively weak ([O III] λ5007/Hβ < 3); and (3) there are often strong emission features from Fe II and high-ionization optical lines. It has recently been discovered that they also have distinctive X-ray properties. *ROSAT* PSPC observations found that the soft X-ray spectra are systematically steeper than in "classical" Seyfert 1 galaxies and that the photon index appears correlated with the optical line width. NLS1s also very frequently exhibit rapid and/or high-amplitude X-ray variability (Boller, Brandt, & Fink 1996; Forster & Halpern 1996 and references therein).

NLS1 observations with *ASCA*, which has better energy resolution and a larger bandpass, find that the steep spectrum in the soft X-ray band is primarily due to a strong soft excess component with characteristic blackbody temperature in the range 0.1–0.2 keV and a relatively weak hard power law. The hard X-ray power-law slope is either remarkably variable (Leighly et al. 1996; Guainazzi et al. 1996) or significantly steeper than found in broad-line Seyfert 1 galaxies (Pounds, Done, & Osborne 1995; Brandt, Mathur, & Elvis 1997). The combination of strong soft excess and steep power law prompted Pounds et al. (1995) to postulate that NLS1s represent the supermassive black hole analog of Galactic black hole candidates in the high state.

2. DATA AND ANALYSIS

We considered all the *ASCA* data from NLS1s in the archive as of 1997 February and in three proprietary data sets, yielding a sample of 16 objects. A standard uniform analysis was applied to all data (see, e.g., Nandra et al. 1997; details in Leighly et al. 1997).

In most cases, a power-law model fitted the spectra poorly, and an additional soft excess model was required. The soft component in these NLS1s is hot and prominent, and a single blackbody is not broad enough to fit the whole energy range from 0.48 keV. A disk blackbody model, which is the sum of blackbodies (Makishima et al. 1986), is broader. Therefore, we fitted a disk blackbody model in the energy band greater than 0.48 keV. However, our discussion of absorption features below does not depend critically on the assumed model of the soft continuum. Fits over a truncated energy band of more than 0.6 keV with a single blackbody give consistent parameters for the absorption features, with comparable χ_ν^2 values.

In many cases, the power-law plus disk blackbody model gave an adequate fit. However, a significant dip remained near 1 keV in the fit residuals from 1H 0707−495, IRAS 13224−3809, and PG 1404+226 (Fig. 1; also see Hayashida 1996; Otani, Kii, & Miya 1996; Comastri, Molendi, & Ulrich 1997). Similar features have been reported in *ROSAT* spectra from Akn 564 (Brandt et al. 1994) and PG 1404+226 (Ulrich-Demoulin & Molendi 1996). Addition of an edge to the model improved the fit by $\Delta\chi^2$/degrees of freedom (d.o.f.) = 33/265, 46/307, and 35/156, significant at a confidence level greater than 99.9%, for 1H 0707−495, IRAS 13224−3809, and PG 1404+226, respectively. For 1H 0707−495 and IRAS 13224−3809, an additional edge reduced the χ^2 by 24 and 11, respectively. The best-fit parameters for these two-edge fits and the single-edge fit for PG 1404+226 are listed in Table 1.

Absorption edges, a signature of highly ionized gas in the line of sight, are commonly found in the X-ray spectra from bright Seyfert 1 galaxies (see, e.g., Reynolds 1997). Oxygen edges from O VII and O VIII at 0.74 and 0.87 keV, respectively, are expected to dominate the absorption profile because of the
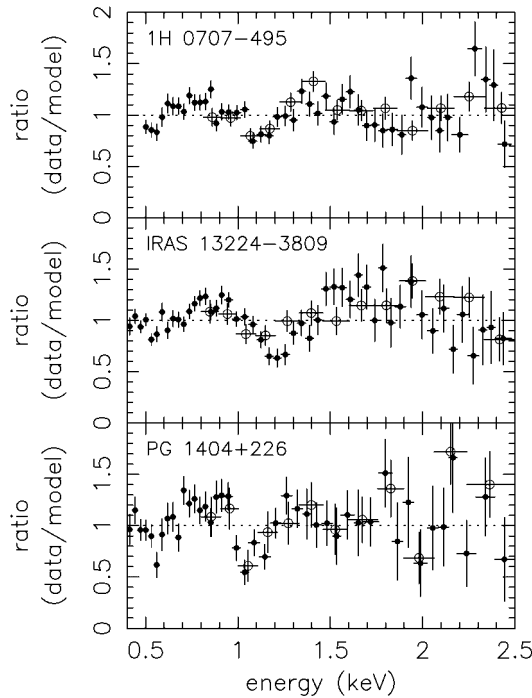

FIG. 1.—Ratio of data to a power-law plus disk blackbody model, showing the edge-like feature around 1 keV in these three objects. Filled and open symbols denote summed SIS and GIS spectra, respectively.

large abundance and cross sections. However, the edges in our objects are found at much higher energies than could be attributed to oxygen in the active galactic nucleus (AGN) rest frame. In this energy range, absorption by neon and iron is expected, but for abundances near solar value, it is difficult to produce deep absorption edges from these elements without

also finding strong oxygen edges. Since neon differs in atomic number from oxygen by only two, its ionization state should not be drastically different. Since both oxygen and neon are plausibly produced predominantly by Type II supernovae, their relative abundances should not vary much. Iron species that could absorb from the L shell are still present when oxygen is nearly fully ionized, but the expected dominant ions have higher energy absorption edges than we find here, near 1.2–1.4 keV.

We can attribute the absorption edges to ionized oxygen if the absorbing material is being accelerated away from the nucleus, similar to broad absorption line galaxies (BALQSOs; for recent reviews, see Weymann 1995; Turnshek 1995). If we identify the observed edges in 1H 0707−495 and IRAS 13224−3809 with O VII and O VIII, we infer an ejection velocity of about −0.2 to −0.3 c (Fig. 2a). This interpretation is supported by the consistency in velocity for both ions. For PG 1404+226, we detect only one edge and infer velocity of either −0.35 or −0.20 c, depending on whether it is due to O VII or O VIII.

Alternatively, the absorption features may be due to resonance line absorption. The *ASCA* SIS detectors have moderate resolution (∼60 eV at 1 keV), and since the lines have a low equivalent width of ∼50 eV, they can be detected only if the velocity dispersion is $\sigma_{vel} \gtrsim 3000$ km s^{-1}. We added "narrow" ($\sigma = 0$) Gaussian lines to the power-law plus disk blackbody model, effectively modeling features narrower than the detector response width. Addition of an absorption line to the disk blackbody plus power-law model reduced the χ^2/d.o.f. by 30/265, 25/303, and 21/151 and the second line by 15/263, 6/301, and 14/149 for 1H 0707−495, IRAS 13224−3809, and PG 1404+226, respectively. Addition of a third line for 1H 0707−495 and IRAS 13224−3809 reduced the χ^2/d.o.f. by 20/261 and 5/298. Details of these multiple-line fits are shown in Table 1. The final χ^2 values are comparable to the edge fit

TABLE 1
SPECTRAL FITTING RESULTS

TARGET	N_H[a] $(10^{21}$ cm$^{-2})$	POWER LAW		BLACKBODY		ABSORPTION FEATURE[b]			χ^2/d.o.f.
		Index	Norm.[c]	kT (keV)	Norm.[d]	Energy (keV)	Depth	ID[e]	
Absorption-Edge Model									
1H 0707−495	$0.63^{+0.71}_{-0.05}$	$2.29^{+0.22}_{-0.21}$	$6.0^{+1.9}_{-1.4}$	$0.20^{+0.02}_{-0.03}$	$0.26^{+0.64}_{-0.09}$	$0.91^{+0.03}_{-0.04}$	0.57 ± 0.20	O VII	318/263
						1.09 ± 0.03	0.67 ± 0.23	O VIII	
IRAS 13224−3809	$0.48^{+0.63}_{-0}$	$1.97^{+0.26}_{-0.25}$	$2.05^{+0.74}_{-0.55}$	$0.19^{+0.02}_{-0.03}$	$0.18^{+0.49}_{-0.07}$	1.03 ± 0.04	$0.60^{+0.28}_{-0.25}$	O VII	339/300
						$1.18^{+0.04}_{-0.03}$	$0.87^{+0.31}_{-0.32}$	O VIII	
PG 1404+226	$0.55^{+1.67}_{-0.34}$	1.67 ± 0.42	$1.5^{+1.1}_{-0.7}$	$0.18^{+0.04}_{-0.05}$	$0.22^{+4.0}_{-0.15}$	1.07 ± 0.03	$1.15^{+0.41}_{-0.44}$	O VII or O VIII	153/151
Absorption-Line Model									
1H 0707−495	1.6 ± 0.08	2.25 ± 0.18	$5.9^{+1.4}_{-1.2}$	0.15 ± 0.02	$2.5^{+6.5}_{-1.8}$	0.98 ± 0.03	30^{+20}_{-15}	N VII	319/261
						$1.12^{+0.03}_{-0.02}$	47^{+18}_{-17}	O VII	
						1.24 ± 0.03	46 ± 20	O VIII	
IRAS 13224−3809	$2.3^{+1.1}_{-0.9}$	1.89 ± 0.23	$1.80^{+0.57}_{-0.46}$	0.13 ± 0.02	$5.3^{+22.2}_{-4.1}$	$1.09^{+0.05}_{-0.03}$	24^{+18}_{-17}	O VII	343/298
						1.23 ± 0.04	48^{+19}_{-24}	O VIII	
						$1.33^{+0.06}_{-0.05}$	46^{+29}_{-31}	?	
PG 1404+226	$2.3^{+1.4}_{-1.2}$	1.68 ± 0.33	$1.53^{+0.75}_{-0.54}$	$0.13^{+0.03}_{-0.02}$	$4.8^{+34.0}_{-4.0}$	1.12 ± 0.03	50^{+29}_{-23}	O VII	150/149
						1.24 ± 0.04	51^{+30}_{-27}	O VIII	

NOTE.—The quoted uncertainties are 90% confidence for two parameters of interest ($\Delta\chi^2 = 4.61$).

[a] Neutral continuum absorption. The lower limit is the Galactic absorption column for the edge fits.

[b] Absorption feature depths are the optical depth τ and the line equivalent width in eV for the edge and line models, respectively. Listed on successive lines are parameters for models with more than one absorption feature.

[c] In units of 10^{-4} photons cm^{-2} s^{-1} at 1 keV.

[d] Multiple blackbody model (Makishima et al. 1986) times $10^3 (R_{IN}/D_{10})^2 \times \cos(\theta)$, where R_{IN} is the inner disk radius in kilometers, D is the distance to the source in units of 10 kpc, and θ is the disk inclination.

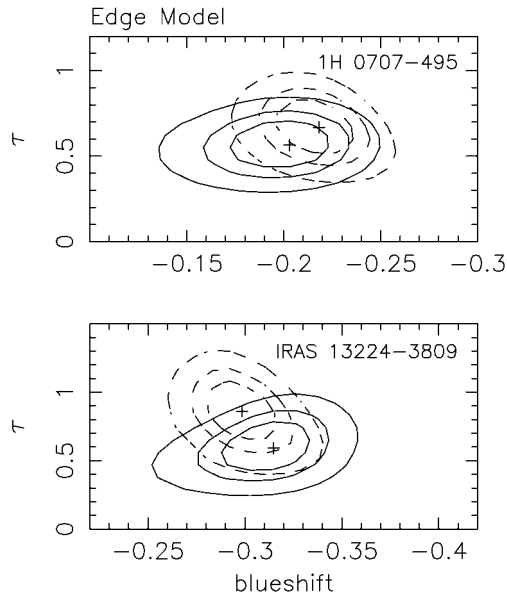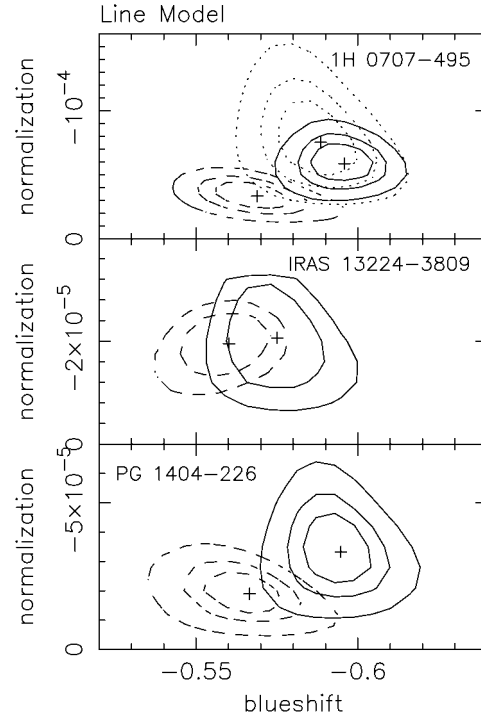[e] Tentative edge/line identification, implying velocities in Fig. 2.

FIG. 2.—When the edges and lines are identified with transitions of oxygen, the ejection velocities from the nucleus can be found. χ^2 contours show 67%, 90%, and 99% confidence intervals; for IRAS 13224−3809, only 67% and 90% confidence are shown. (a) Absorption-edge fits; (b) absorption-line fits. Solid, dashed, and dotted lines indicate O VII, O VIII, and N VI, respectively.

results, so we cannot distinguish these models statistically. Note that the two lines present in all spectra are consistent in energy from object to object, although the differences in cosmological redshift ($z = 0.041$, 0.067, and 0.098 for 1H 0707−495, IRAS 13224−3809, and PG 1404+226, respectively) imply a difference of 50 eV in observed energy. Assuming that the absorber is completely opaque and fitting with the XSPEC *notch* model (equivalent to a very saturated absorption line) gives a velocity profile FWHM of ~10,000–14,000 km s^{-1}, similar to that found in BALQSOs. Resonance absorption is expected to be strong in hydrogen-like and helium-like atoms, and the ratios of the energies should be the same for every element. Again, we can plausibly identify the two common lines in all spectra as O VII and O VIII at ~0.565 and 0.651 keV, respectively. A lower energy line in the 1H 0707−495 spectrum is plausibly N VII at 0.498 keV, while a higher energy line in the IRAS 13224−3809 spectrum has no clear identification. These line identifications imply consistent ejection velocities, near −0.57 c (Fig. 2b). Absorption edges should accompany the resonance absorption lines (Madejski et al. 1993). Adding O VII and O VIII absorption edges to the model with energies fixed at the values predicted if $v/c = -0.57$, we find that the optical depths τ are consistent with zero, and the $\Delta\chi^2 = 4.61$ upper limits were 0.27, 0.68, and 0.50 for O VII and 0.32, 0.13, and 0.26 for O VIII, for 1H 0707−495, IRAS 13224−3809, and PG 1404+226, respectively. In § 3 we show that estimations of the column densities derived from these upper limits are consistent with those from the absorption-line equivalent widths.

As noted above, the measured edge energies seem inconsistent with those expected from iron-L species. However, iron is a complex ion potentially producing a complex absorption profile that might fit these moderate-resolution spectra. We used

a power-law plus disk blackbody model, transmitted through an ionized absorber in the AGN rest frame with iron abundance free (Magdziarz & Zdziarski 1995). In this model, the electron temperature T and the ionization parameter ξ are both free parameters, and we chose two representative values, $T_{\text{low}} = 3 \times 10^4$ K and $T_{\text{high}} = 3 \times 10^5$ K. These models produced a worse fit overall compared with the models described above and required rather large iron overabundances. For $T = T_{\text{low}}$, we obtained iron abundance lower limits of 15, 29, and 17 times solar values with $\Delta\chi^2$/d.o.f. = 11/264, 13/301, and 6/150, and for $T = T_{\text{high}}$, we obtained iron abundance best-fit values of 3.9, 7.3, and 12.8 with $\Delta\chi^2$/d.o.f. = 0/264, 12/301, and 7/150 for 1H 0707−495, IRAS 13224−3809, and PG 1404+226, respectively. Iron enhancements up to 10 with respect to oxygen might be expected in some cases, but probably not as large as 20 (Hamann & Ferland 1993). A high iron abundance could not be responsible for the strong Fe II emission in NLS1s, because the resulting cooler temperature decreases the number of Fe$^+$ ions while the optical depth to escaping Fe II increases (see, e.g., Joly 1993).

In summary, we tried to explain the 1 keV features using three different models. Both absorption edges and lines produced a good fit that could not be distinguished statistically. The iron overabundance model generally gave a poorer fit.

3. DISCUSSION

The outflow velocities of 0.2–0.6 c inferred in these objects are very large, larger than those observed the UV spectra of BALQSOs. Such large velocities could be difficult to identify in the UV band, because the prominent C IV line would be shifted out of the bandpass or into the Lyα forest, where it might be hard to distinguish. Also, very large velocity disper-

sions with moderate column densities might result in lines so broad that they blend in with the continuum.

It is beyond the scope of this Letter to speculate on the mechanism required to accelerate material to these very large velocities, but it is interesting to note that the velocity implied by the edge fits is close to that seen in the Galactic jet object SS 433 of 0.26 c and to the terminal velocity predicted by "line locking" of 0.28 c (Shapiro, Milgrom, & Rees 1986). The larger velocities implied by the absorption-line fits are intriguingly close to the energy of a particle in circular orbits around a Kerr black hole (see, e.g., Shapiro & Teukolsky 1983). However, it seems difficult to relate this fact to a physical outflow mechanism.

We obtain lower limits on the equivalent hydrogen column. For the absorption-edge model, assuming cross sections of 2.8 and 0.98×10^{-19} cm^{-2} for O VII and O VIII, respectively, and an oxygen abundance relative to hydrogen of 8.51×10^{-4}, the O VII+O VIII equivalent hydrogen column densities are in the range of 0.4–1.3×10^{22} cm^{-2}. For the absorption lines, assumed to be on the linear part of the curve of growth, oscillator strengths of 0.694 and 0.416 for O VII and O VIII were used, giving O VII+O VIII equivalent hydrogen column densities of 1.6–2.1×10^{21} cm^{-2}. In each case, the column density upper limits on the absorption edges predicted to accompany these absorption lines were larger, which shows that this model is viable. While estimation of the ionization parameter depends on the input continuum and is beyond the scope of this Letter, we note that the O VIII column is always larger than the O VII column, which implies a fairly high ionization parameter.

Rest-frame absorption features in the X-ray spectra of broad-line hard X-ray–selected AGNs are common (Reynolds 1997), plausibly arising in the same material as $z_{em} \approx z_{ab}$ absorption lines found in the UV band (see, e.g., Mathur, Elvis, & Wilkes 1995). These "associated" absorption features may be related to the broad UV absorption lines seen in higher luminosity objects (see, e.g., Kolman et al. 1993). Evidence suggests that some aspect of the NLS1 central engine is significantly different compared with broad-line objects; for example, they may be characterized by a higher accretion rate relative to Eddington luminosity (Pounds et al. 1995). The rapid, higher amplitude, and perhaps characteristically nonlinear X-ray variability may be evidence for strong relativistic effects (Boller et al. 1997; Leighly et al. 1997). These results may indicate a higher level of activity relative to the black hole mass in NLS1s, and strong relativistic outflows might be expected.

The blueshifted absorption features discussed here are reminiscent of those found in the UV spectra of broad absorption line quasars. A connection between NLS1s and BALQSOs may be quite reasonable, considering that they have many optical emission line and broadband continuum properties in common. Many NLS1s and BALQSOs show strong or extreme Fe II emission and weak [O III] emission. Objects that have the strongest Fe II emission and weakest or no [O III] emission tend to be either low-ionization BALQSOs or NLS1s (Boroson & Meyers 1992; Turnshek et al. 1997; Lawrence et al. 1997). Many NLS1s and low-ionization BALQSOs have red optical continuum spectra and relatively strong infrared emission (Boroson & Meyers 1992; Moran, Halpern, & Helfand 1996; Turnshek 1997). Finally, both classes are predominantly radio quiet (Stocke et al. 1992; Ulvestad, Antonucci, & Goodrich 1995).

An interesting possibility is that low-ionization BALQSOs and NLS1s have a common parent population (see, e.g., Lawrence et al. 1997). If so, perhaps objects with intermediate properties between NLS1s and low-ionization BALQSOs should exist. It was recently reported that NLS1 IRAS 13349+2438 has UV broad absorption lines (Turnshek 1997). But while most BALQSOs are X-ray quiet, this object is a bright soft X-ray source and has the very steep hard X-ray spectrum and rapid X-ray variability characteristic of NLS1s (Brinkmann et al. 1996).

REFERENCES

Boller, Th., Brandt, W. N., Fabian, A. C., & Fink, H. 1997, MNRAS, 289, 393
Boller, Th., Brandt, W. N., & Fink, H. 1996, A&A, 305, 53
Boroson, T. A., & Meyers, K. A. 1992, ApJ, 397, 442
Brandt, W. N., Fabian, A. C., Nandra, K., Reynolds, C. S., & Brinkmann, W. 1994, MNRAS, 271, 958
Brandt, W. N., Mathur, S., & Elvis, M. 1997, MNRAS, 285, 25
Brinkmann, W., Kawai, N., Ogasaka, Y., & Siebert, J. 1996, A&A, 316, 9
Comastri, A., Molendi, S., & Ulrich, M. H. 1997, X-Ray Imaging and Spectroscopy of Cosmic Hot Plasmas, ed. F. Makino & K. Mitsuda (Tokyo: Univ. Acad. Press), 279
Forster, K., & Halpern, J. P. 1996, ApJ, 468, 565
Goodrich, R. W. 1989, ApJ, 342, 224
Guainazzi, M., Mihara, T., Otani, C., & Matsuoka, M. 1996, PASJ, 48, 781
Hamann, F., & Ferland, G. 1993, ApJ, 418, 11
Hayashida, K. 1996, IAU Colloq. 159, Emission Lines in Active Galaxies: New Methods and Techniques, ed. B. M. Peterson, F.-Z. Cheng, & A. S. Wilson (San Fransisco: ASP), 40
Joly, M. 1993, Ann. Phys., 18, 241
Kolman, M., Halpern, J. P., Martin, C., Awaki, H., & Koyama, K. 1993, ApJ, 403, 592
Lawrence, A., Elvis, M., Wilkes, B. J., McHardy, I., & Brandt, N. 1997, MNRAS, 286, 879
Leighly, K. M., Mushotzky, R. F., Yaqoob, T., Kunieda, K., & Edelson, R. 1996, ApJ, 469, 14
Leighly, K. M., et al. 1997, in preparation
Madejski, G. M., et al. 1993, in BBXRT: A Preview to Astronomical X-Ray Spectroscopy in the '90s, ed. P. J. Serlemitsos, & S. Shrader (Greenbelt: NASA/GSFC), 63

Magdziarz, P., & Zdziarski, A. A. 1995, MNRAS, 273, 837
Makishima, K., et al. 1986, ApJ, 308, 635
Mathur, S., Elvis, M., & Wilkes, B. 1995, ApJ, 452, 230
Moran, E. C., Halpern, J. P., & Helfand, D. J. 1996, ApJS, 106, 341
Nandra, K., George, I. M., Mushotzky, R. F., Turner, T. J., & Yaqoob, T. 1997, ApJ, 476, 70
Otani, C., Kii, T., & Miya, K. 1996, in MPE Rep. 263, Röntgenstrahlung from the Universe, ed. H. U. Zimmermann, J. Trümper, & H. Yorke, 491
Pounds, K. A., Done, C., & Osborne, J. 1995, MNRAS, 277, L5
Reynolds, C. S. 1997, MNRAS, 286, 513
Shapiro, P. R., Milgrom, M., & Rees, M. J. 1986, ApJS, 60, 393
Shapiro, S. L., & Teukolsky, S. A. 1983, Black Holes, White Dwarfs, and Neutron Stars (New York: Wiley)
Stocke, J. T., Morris, S. L., Weymann, R. J., & Foltz, C. B. 1992, ApJ, 396, 487
Turnshek, D. A. 1995, in QSO Absorption Lines, ed. G. Meylan (Berlin: Springer), 223
———. 1997, in Mass Ejection from Active Galactic Nuclei, ed. R. J. Weyman, N. Arav, & I. Shlosman (San Francisco: ASP), in press
Turnshek, D. A., Monier, E. M., Sirola, C. J., & Espey, B. R. 1997, ApJ, 476, 40
Ulrich-Demoulin, M. H., & Molendi, S. 1996, ApJ, 457, 77
Ulvestad, J. S., Antonucci, R. R. J., & Goodrich, R. W. 1995, AJ, 109, 81
Weymann, R. J. 1995, in QSO Absorption Lines, ed. G. Meylan (Berlin: Springer), 213